Terminal minihelix, a novel RNA motif that directs polymerase III transcripts to the cell cytoplasm - Terminal minihelix and RNA export

C. Gwizdek, Edouard Bertrand, Catherine Dargemont, Jean-Claude Lefebvre, Jean-Marie Blanchard, Robert H. Singer, Alain Doglio

THE JOURNAL OF BIOLOGICAL CHEMISTRY
Vol. 276, No. 28, Issue of July 13, pp. 25910–25918, 2001

Printed in U.S.A.

Terminal Minihelix, a Novel RNA Motif That Directs Polymerase III Transcripts to the Cell Cytoplasm

TERMINAL MINIHELIX AND RNA EXPORT*

Received for publication, January 18, 2001, and in revised form, April 10, 2001
Published, JBC Papers in Press, May 7, 2001, DOI 10.1074/jbc.M100493200

Carole Gwizdek‡§¶, Edouard Bertrand¶‖, Catherine Dargemont§, Jean-Claude Lefebvre‡, Jean-Marie Blanchard‖, Robert H. Singer**, and Alain Doglio‡ ‡‡**

*From the ‡U526-Laboratoire de Virologie, Faculté de Médecine, Avenue de Valombrose, 06107 Nice cedex 2, France, the ‖Institut de Génétique Moléculaire de Montpellier, 34293 Montpellier Cedex 5, France, the **Department of Anatomy and Structural Biology and Cell Biology, Albert Einstein College of Medicine, Bronx, New York 10461, and the §Laboratoire de Transport Nucléocytoplasmique, Institut Jacques Monod, 2 place Jussieu, 75251 Paris cedex 5, France*

Determining the *cis*-acting elements controlling nuclear export of RNA is critical, because they specify which RNA will be selected for transport. We have characterized the nuclear export motif of the adenoviral VA1 RNA, a small cytoplasmic RNA transcribed by RNA polymerase III. Using a large panel of VA1 mutants in both transfected COS cells and injected *Xenopus* oocytes, we showed that the terminal stem of VA1 is necessary and sufficient for its export. Surprisingly, we found that the nucleotide sequence within the terminal stem is not important. Rather, the salient features of this motif are its length and its relative position within the RNA. Such stems thus define a novel and degenerate cytoplasmic localization motif that we termed the minihelix. This motif is found in a variety of polymerase III transcripts, and cross-competition analysis in *Xenopus* oocytes revealed that export of one such RNA, like hY1 RNA, is specifically competed by VA1 or artificial minihelix. Taken together these results show that the minihelix defines a new *cis*-acting export element and that this motif could be exported via a novel and specific nuclear export pathway.

Correct intracellular localization of RNA is essential for its function and can be utilized by the cell to regulate gene expression. Cytoplasmic or nuclear localization of RNA results from a balance between two opposing mechanisms, nuclear retention and transport through the nuclear pores (1–3). Analyses of RNA export in *Xenopus* oocytes have shown that the export machinery relies on saturable factors (4–6), and cross-competition experiments have revealed the existence of only a few transport pathways, roughly corresponding to major functional classes of RNA: rRNA, mRNA, snRNA, and tRNA.

Many essential transport factors have now been identified, such as Ran, exportins of the importin β family, and TAP (7–10). Exportins and TAP are transporters that shuttle between the nucleus and the cytoplasm to transport a new cargo at each cycle. They can bind their cargo directly or via adaptor molecules. Ran is a small GTPase able to switch between GDP- and GTP-bound states, Ran-GTP is formed in the nucleus, whereas conversion into Ran-GDP is catalyzed in the cytoplasm. RCC1, the Ran GDP exchange factor (RanGEF), is exclusively nuclear whereas the Ran GTPase-activating protein (RanGAP) as well as the co-stimulatory factors RanBP1 and RanBP2 are cytoplasmic or at the cytoplasmic face of the nuclear pore complex. This is thought to provide a gradient of Ran within the cell with RanGTP in the nucleus and RanGDP in the cytoplasm. Exportins bind their substrates in a RanGTP-dependent way and in the cytoplasm, stimulation of GTP hydrolysis on Ran triggers dissociation of the cargo from its receptor. A well characterized example of a Ran-dependent export pathway is illustrated by the tRNA export. RanGTP, but not RanGDP, can form, in the nucleus, a stable trimeric complex containing Ran, tRNA, and the tRNA exportin, Xpo-t, (11–13). Following translocation through the nuclear pores, the cytoplasmic Ran-GTPase-activating proteins promote GTP hydrolysis and disassembly of the complex (14, 15). The tRNA is thus released, and the other factors can be recycled for another round of export.

Despite our knowledge of export mechanisms, the actual RNA elements that promote export are still not well characterized. These elements are however critical because they are responsible for the specificity of transport; they are the initial trigger of the export process, and they determine which RNA will be selected from the nuclear RNA population. To date, the best example characterized is that of snRNAs, for which the export determinant was shown to consist of the 5′-cap structure and is thus identical for all the RNAs of this family (16). A common export determinant probably also exists for tRNAs because Xpo-t recognizes a conserved feature of the structure that is formed by acceptor and T stems (11, 17, 18). The export determinants of other classes of RNA are not known. In the case of mRNAs, a variety of sequences could be involved in addition to the 5′-cap and the poly(A) tail (1, 19–21). Indeed, many mRNA-binding proteins shuttle between the nucleus and the cytoplasm (22, 23, 24) and could be adaptors between mRNA and the export machinery.

As suggested by these examples, it is likely that cytoplasmic RNAs of different classes bear specific *cis*-acting export elements, many of them remaining uncharacterized. In the present study, we focused on polymerase III transcripts (pol III),[1] and we have analyzed in detail the adenovirus VA1 RNA (VA1). VA1 is a small viral RNA, which accumulates in large amounts

* This work was supported by the Agence Nationale de Recherche sur le SIDA (ANRS), Sidaction, the Boris Vlasov Fundation (Monaco), ARC grant 9043, and National Institutes of Health Grants GM54887 and 57071. The costs of publication of this article were defrayed in part by the payment of page charges. This article must therefore be hereby marked "*advertisement*" in accordance with 18 U.S.C. Section 1734 solely to indicate this fact.

¶ Both authors contributed equally to this work.

‡‡ To whom correspondence should be addressed. Tel.: 33 4-93-37-7678; Fax: 33 4-93-81-5484; E-mail: doglio@unice.fr.

[1] The abbreviations used are: pol III, polymerase III; nt, nucleotide.

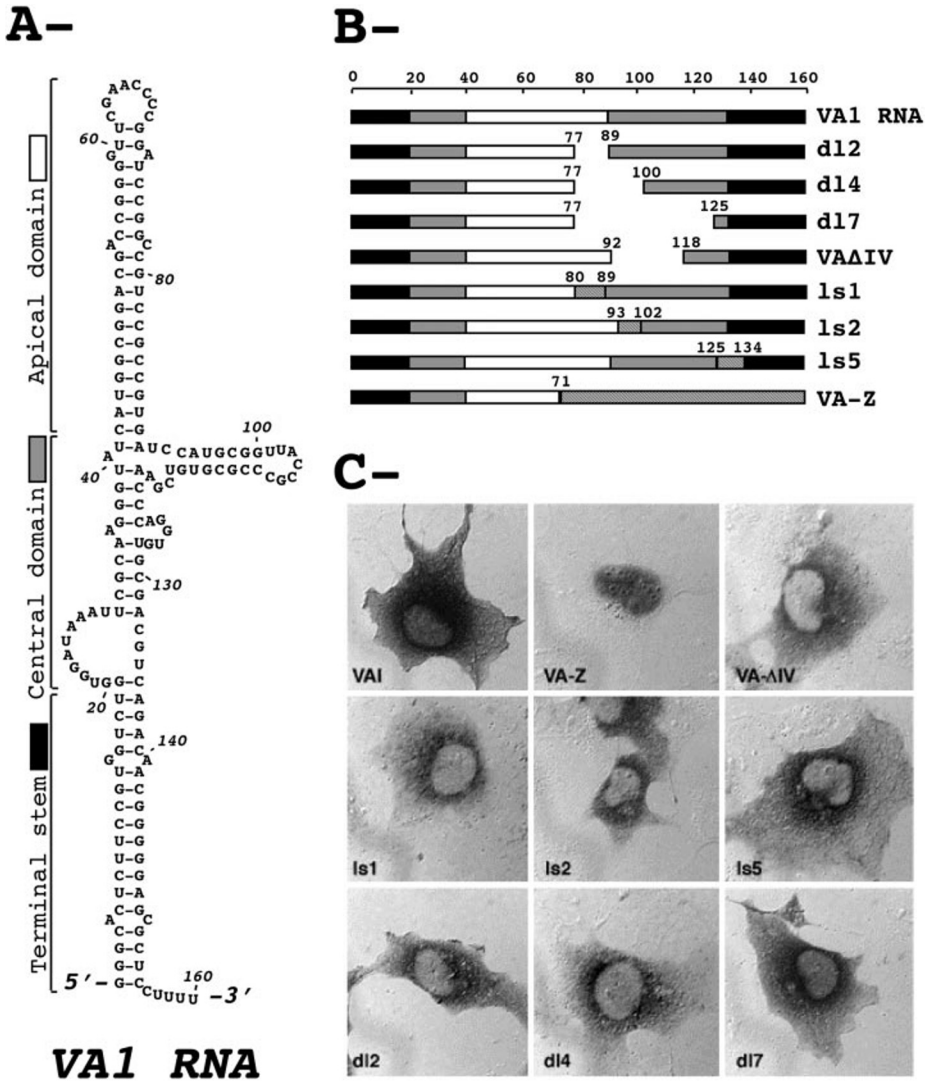

FIG. 1. **Nuclear export of VA1 does not require its central and apical domains.** *A,* sequence and secondary structure of the Ad2 VA1 RNA. The apical, central, and terminal domains are indicated by *large brackets*. *B,* the VA1 mutants. Apical, central, and terminal domains are figured using *black*, *gray*, and *white boxes*, respectively. The position of the deletions (*dl*) are indicated by *gaps*, whereas linker scanning mutants (*ls*) are pictured by *hatched lines* (52). The VAΔIV mutant lacks the entire central domain (30). *C,* intracellular localization of VA1 RNA mutants. COS1 cells were transiently transfected with the indicated plasmids, and the localization of the resulting RNA was analyzed by *in situ* hybridization. Each field represents 100 μm and shows a representative cell (see Table I for quantifications).

in the cytoplasm of adenovirus-infected cells (25, 26). Its function is to inhibit the double-stranded-dependent kinase, PKR, which otherwise blocks translation of the viral mRNAs (27). Our study led us to identify a new *cis*-acting RNA export motif that we termed the minihelix motif. Interestingly, this motif is encountered in a large family of small viral and cellular transcripts, which all are transcribed by pol III.

EXPERIMENTAL PROCEDURES

Plasmid Constructions—The sequences of U1ΔSm, U6Δss, hY1, and $tRNA^{Phe}$ have been previously described (16, 28, 29). The different mutations introduced into the terminal stem of the VAΔIV gene were obtained through the specific annealing of two complementary synthetic oligonucleotides and cloned into blunted restriction sites of the VAΔIV (*Eco*RV and *Eco*47III) (30). Artificial sequences were obtained by cloning polymerase chain reaction fragments downstream of the human U6 promoter. All constructs containing artificial sequences were derived from the pU6+1 plasmid (31). All relevant sequences are shown in the figures, except for the loop of the artificial RNAs (base number 2321–2364 of LacZ, starting from the ATG).

Recombinant Proteins—Purified recombinant *Schizosaccharomyces pombe* Rna1p and RanBP1 were provided by A. Wittinghofer (Max Planck Institute, Dormund, Germany). RanQ69L-GTP was expressed and purified essentially as described (54) using an expression vector provided by C. Dingwall (Stony Brook, N.Y.).

Cell Culture—Monkey COS1 cells were grown at 37 °C in Dulbecco's modified Eagle's medium containing 10% calf fetal serum. Cells were transformed by the calcium-phosphate co-precipitation procedure and analyzed 24 h after transfection (31).

In Vitro Transcriptions—Transcription reactions were performed on polymerase chain reaction products using the Ampliscribe T7 transcription kit (Epicentre Technologies) (see also Ref. 30). Labeled RNAs were synthesized by adding 80 μCi of [^{32}P]UTP (3000 Ci/mmol), and unincorporated nucleotides were removed by gel filtration. Capped U1ΔSm RNA was transcribed in the presence of 3 mM of $m^7G(5')pppG$. The sequence of the RNA injected into *Xenopus* oocytes corresponded exactly to the one expressed in mammalian cells, except that the first three bases (GUC) were replaced by GGG to allow for an efficient *in vitro* transcription. The complementary bases in the RNA structure were also modified to compensate for these changes.

Oocyte Injection—Nuclear injections were performed in *Xenopus* oocytes as previously described (32), with a total volume of 20 nl of RNA mixture per nucleus. To control nuclear injection, samples were mixed with trypan blue (0.5 mg/ml). After nuclear injection, oocytes were incubated at 19 °C for the indicated time in modified bath medium, then transferred into ice-cold 1% trichloroacetic acid. After manual dissection, only oocytes with blue nuclei were used for further analysis. Nuclear and cytoplasmic fractions were homogenized in solubilization buffer (50 mM Tris-HCl, pH 7.5, 5 mM EDTA, 300 mM NaCl, and 0.5% SDS). Samples were then shaken for 30 min at 4 °C before digestion by proteinase K (2 mg/ml) for 30 min at 56 °C. RNAs were purified using conventional molecular biology techniques (phenol extraction and ethanol concentration) then analyzed on denaturing polyacrylamide gels and autoradiographed. For each sample, five oocytes were pooled and 2 oocyte equivalents were loaded by lane. As artificial minihelices are highly structured RNAs, they migrate faster than expected and Stem17 (90 nt) migrates faster than $tRNA^{Phe}$ (76 nt) unless gels are prerun for 30 min at 25 watts before loading. When indicated results were quantified using the Bioprint acquisition system and Bioprofil program (Vilbert Lourmat, France).

In Situ Hybridization—In situ hybridization was performed as pre-

TABLE I
Quantification of the localization of the different constructs used in this study and characterization of their intracellular stability

RNA[a]	*In situ* localization in COS1 cells[b]			Nuclear export in *Xenopus* oocytes[c]	Half-life[d]
	Cytoplasmic	Nuclear	Intermediate		
	%	%	%	%	*h*
VA1	79	13	8	68	nd
VAΔIV	80	4	16	44	5.3
Mut0	69	10	21	nd	6.5
Mut1	74	8	18	nd	nd
Mut2	77	9	13	nd	nd
Mut3	77	2	21	nd	7.5
Mut4	2	76	22	nd	5.3
Mut5	1	95	4	6	3.2
Mut6	12	42	46	nd	6.0
Mut10	5	78	17	0.4	0.6
Stem20	78	15	15	26	3.0
Stem17	85	5	10	15	7.0
Stem14	12	45	43	nd	nd
Stem12	7	73	24	0	3.7
MM1	12	43	48	nd	nd
MM3	2	85	14	0	nd
Xt8	73	7	20	nd	nd
Xt18	6	81	13	nd	nd
Stem-3A	68	10	22	nd	nd
Stem-6A	72	9	19	nd	nd

[a] The different VA1 RNA mutants tested are described in detail in Figs. 2 and 4.
[b] COS1 cells were transfected with plasmids encoding the indicated RNA, and their intracellular distribution was analyzed by *in situ* hybridization. Cells were scored by eye examination and counted as "cytoplasmic" if 75% or more of the signal was in the cytoplasm, as "nuclear" if 75% or more of the signal was in the nucleus, and as "intermediate" in all other cases. The numbers represent the percent of cells showing either a cytoplasmic, a nuclear, or an intermediate signal. The numbers were averaged from three independent experiments, and at least 100 positive cells were counted each time. The standard deviation was lower than 15% in all cases.
[c] Radiolabeled RNAs were injected in the nucleus of *Xenopus* oocytes and after incubation at 19 °C for 3 hours were extracted from nuclear and cytoplasmic fractions and analyzed by polyacrylamide gel electrophoresis as shown in Fig. 3*B*. Results were quantified using the Bioprint acquisition system and Bioprofil program (Vilbert Lourmat, France) and expressed as the percent of RNA located in the cytoplasmic fraction. The numbers were averaged from at least two independent experiments. nd, not determined.
[d] 293 cells were transfected with plasmids encoding the indicated mutants and then treated (or not) with actinomycin D. At different times, RNAs were extracted, and their expression level was quantified by Northern blot analysis. The intracellular stability (half-lives) determination was calculated with reference to the zero time sample. Half-lives were the average of 2 or 3 independent experiments. nd, not determined.

viously described (30, 33) with digoxigenin-labeled RNA probes and revealed with alkaline phosphatase-conjugated antibodies.

RESULTS

The Terminal Stem of VA1 Determines Its Intracellular Localization—VA1 has been previously dissected into three different functional domains (Refs. 25, 34–36 and Fig. 1*A*): an apical stem-loop, required for PKR binding; a central domain, responsible for PKR inhibition; and a terminal stem, which brings together the 5′- and 3′-ends of the RNA. In previous studies, several VA1 mutants, having well defined secondary structure, had been generated (30, 34–36). The mutations were introduced in the apical or central domains but maintained an intact terminal stem (Fig. 1*B*). Intracellular localization of these VA1 mutants was analyzed in transiently transfected COS1 cells using *in situ* hybridizations. These mutant RNAs (dl2, dl4, dl7, VAΔIV, ls1, ls2, ls5) accumulated in large amounts in the cytoplasm, similarly to the parental VA1 (Fig. 1*C* and see Table I for quantifications). Thus, neither the apical domain nor the central domain appeared to be required for the cytoplasmic localization of VA1. Some sequences were, however, necessary, because a construct for which the 3′-half of VA1 was replaced by some unrelated lacZ sequence remained nuclear (Fig. 1*C*, *VA-Z*).

To test whether the terminal stem was necessary for export, we created a new set of mutants. Mutations were inserted into a VA1 derivative (VAΔIV) that despite the lack of the central domain localized in the cytoplasm (Refs. 30, 37 and Fig. 1*C*). As shown in Fig. 2*A*, some mutations introduced mismatches within the stem (Mut4, Mut5, Mut6), whereas others interrupted it (Mut8, Mut10). It was expected that the design of these mutations might profoundly affect the secondary structure of the VA1 terminal stem. Mut4, Mut5, and Mut10 were not exported to the cytoplasm and remained mostly nuclear, while Mut6 and Mut8 showed an intermediary phenotype (Fig. 2*B* and see Table I for quantifications). It thus appeared that mutations affecting the terminal stem structure had profound effects on VA1 cytoplasmic localization.

Changes in either the export process itself, or in RNA stability, can affect the steady-state cellular localization of RNA. Indeed, some mutations could selectively impair VA1 stability in the cytoplasm and to result in a global change of nucleocytoplasmic partitioning. Steady-state expression levels, of all the tested VA1 RNA mutants, were however very similar in different cell types (293, COS1) as demonstrated by Northern blot analysis of transiently transfected cells (data not shown). We also measured VA1 RNA mutant half-life in 293 cells treated with actinomycin D (Table I). With the exception of Mut10, which was significantly less stable (half-life: 40 min), half-lives of all the VA1 mutants were very similar, independent of the nuclear or the cytoplasmic localization of the mutant. Half-lives of these RNAs were similar to that of the parental VA1 ranging between 2.5 and 6.5 h (Table I). Thus, it appeared that the terminal stem was required for export *per se* and not for cytoplasmic RNA stability.

The Terminal Stem of VA1 Is a Nuclear Export Element—To unambiguously prove that the VA1 terminal stem was a *cis*-acting export element, we turned to the model of *Xenopus* oocyte, which allows direct kinetic analyses of transport. Different radiolabeled RNAs were injected into oocyte nuclei, and their nucleocytoplasmic distribution was analyzed at different times after injection (Fig. 3*A*). Consistent with earlier findings, $tRNA^{phe}$ and hY1 RNA were gradually exported to the cytoplasm, whereas a U6Δss RNA remained nuclear (6, 38, 39). VA1 and VAΔIV were also gradually exported, and about half of the RNA was detected in the cytoplasm 3 h after nuclear injection. Subsequently, the export of several of the VA1 RNA

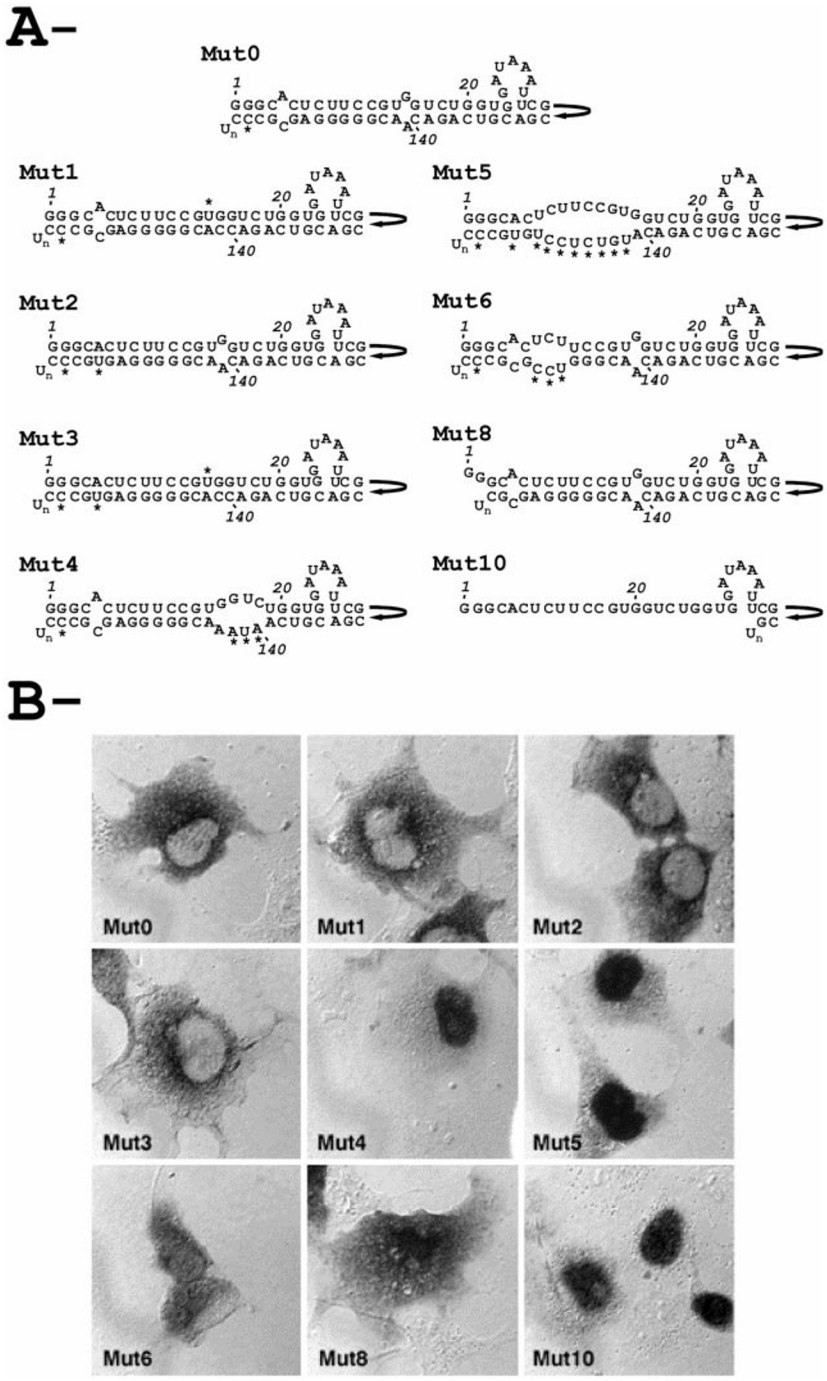

FIG. 2. **Nuclear export of VA1 requires an intact terminal stem.** *A,* structures of the VA1 terminal stem mutants: only the terminal stem is pictured (from base 1 to 33 and from base 130 to 160, respectively, see Fig. 1), and the mutations are indicated by *asterisks*. *B,* the VA1 terminal stem is required for its export. COS1 cells were transiently transfected with the indicated plasmids, and the localization of the resulting RNA was analyzed by *in situ* hybridization. Each field represents 100 μm and shows a representative cell (see Table I for quantifications).

mutants, previously used in COS1 cells (see Fig. 2), was analyzed in *Xenopus* oocyte (Fig. 3*B*). VA1 RNA mutants having no terminal stem (Mut10) or a strong alteration of the stem structure (Mut5), and which were shown to remain nuclear in COS1 cells (Fig. 2*B*), were also not exported in *Xenopus* (Fig. 3*B*). This lack of cytoplasmic accumulation did not result from a specific degradation in the oocyte cytoplasm, because decay of the total injected RNA was minimal and also similar for exported RNAs (Fig. 3*B*).

Previous studies in *Xenopus* oocytes have shown that all known RNA export pathways can be specifically and independently saturated by an excess of substrate RNA. As shown in Fig. 4, co-injection of an excess of VA1 completely inhibited the nuclear export of radiolabeled VA1 (*lanes 5* and *6 versus lanes 2* and *3*). The competition was specific because the export of U1ΔSm was not affected whereas, conversely, an excess of U1ΔSm did not compete for VA1 export (*lanes 8* and *9*). Taken together, these experiments showed that the VA1 terminal stem was sufficient and necessary to promote the nuclear export of the VA1 both in mammalian cells and *Xenopus* oocyte through a saturable export pathway.

Terminal Stems of Artificial Sequences Are Exported to Cell Cytoplasm—A comparative analysis of all VA1 sequences from human and simian adenoviruses available in databases showed that the overall structure of the VA1 terminal stem was well conserved. This stem was characterized by base pairing of the 5′- and 3′-RNA termini over 20 bases and the presence of two mismatches regularly spaced (Fig. 1*A* and Ref. 25). To determine whether the mismatches were important for export, we converted them into base pairs (Mut1–3, Fig. 2*A*). After transfection in COS1 cells, these mutants localized in the cytoplasm as efficiently as VA1 (Fig. 2*B*). A further analysis of

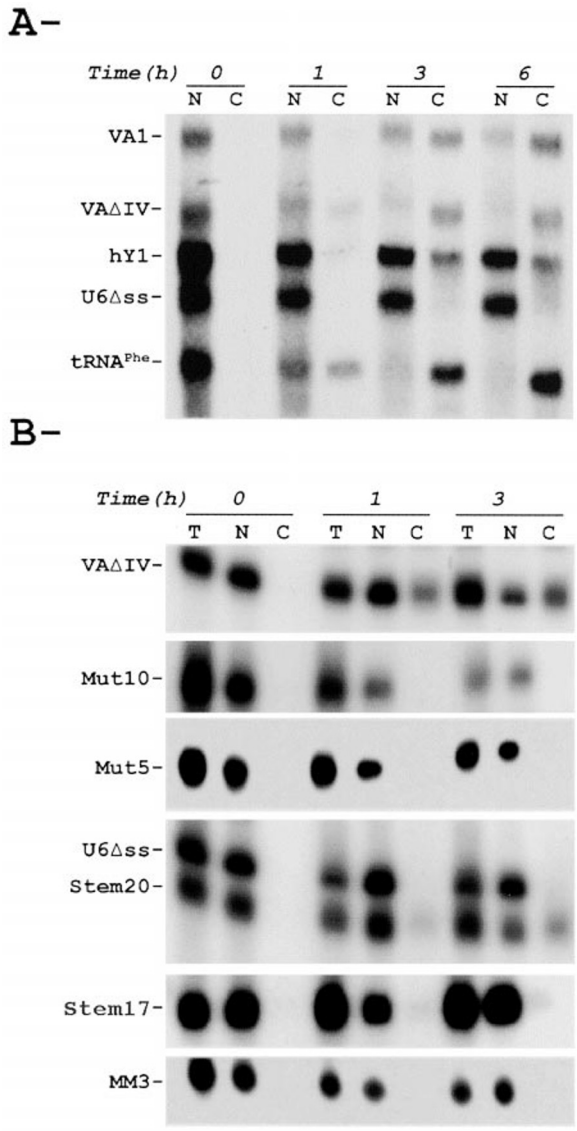

FIG. 3. **Analysis of RNA export in *Xenopus laevis* oocytes.** *A*, nuclear export of VA1 and VAΔIV RNAs. A mixture of 1.5 fmol of ^{32}P-labeled VA1, VAΔIV, hY1, U6Δss, and tRNA^{Phe} was injected into oocyte nuclei. After the indicated time at 19 °C, nuclear and cytoplasmic RNA (*N* and *C*, respectively) were extracted and analyzed by polyacrylamide gel electrophoresis in denaturing conditions. *B*, terminal stems are required to export VA1 or artificial minihelices. The structure of the different VA1 RNA mutants used in this experiment (*Mut10* and *Mut5*) is shown in Fig. 2, and the artificial RNAs (*Stem20* and *Stem17*) are depicted in Fig. 5. 1.5 fmol of the indicated radiolabeled RNAs were injected into oocyte nuclei. After the indicated time at 19 °C, total (*T*), nuclear (*N*), and cytoplasmic (*C*) RNA were treated as described in *A*.

VA1 sequences failed to reveal a particular consensus motif in the sequence of the terminal stem (data not shown). This suggested that the primary sequence of the stem was not important, as long as its structure was conserved. To positively prove this point, we created several artificial RNAs (Fig. 5*A*). These RNAs were derived from the LacZ sequence, and they were chosen to show no similarity to the primary sequence of VA1. Even though they contained no natural sequences, they were designed to form a terminal stem mimicking that of VA1 at the structural level. In a first step, two RNAs were generated, that formed a terminal stem of either 20 or 17 bases (Fig. 5*A*, *Stem20* and *Stem17*). Because the *VA1* gene contains an intragenic promoter (40), another pol III promoter, the human U6 promoter, was used to express Stem20 and Stem17 in COS1 cells. As shown in Fig. 5*B*, Stem20 and Stem17 efficiently accumulated in the cytoplasm of transfected cells. In addition, injection of Stem20 and Stem17 in *Xenopus* oocyte nuclei showed that these artificial RNAs were also exported in this system, similar to VAΔIV (Figs. 3*B* and 4). Interestingly, export of Stem17 appeared to be a saturable process because it was blocked by an excess of Stem17 (Fig. 4, *lane 12 versus lane 3*). Furthermore, export of Stem17 was also inhibited by an excess of VA1 competitor (Fig. 4, *lane 6 versus lane 3*), and, reciprocally, export of VA1 was blocked by an excess of Stem17 (Fig. 4, *lane 12 versus lane 3*). These competitions were specific because export of U1ΔSm was not affected.

These results demonstrated that artificial RNAs displaying a terminal stem with structural features similar to the one of VA1 were localized in the cytoplasm of both mammalian cells and *Xenopus* oocytes. Remarkably, no specific sequences appeared to be required within the terminal stem, they thus represented a highly degenerate cytoplasmic localization motif that we termed the minihelix. Furthermore, cross-competition experiments indicated that artificial terminal stems and VA1 likely shared the same export pathway.

Structural Requirements in Minihelices for RNA Export—The apparent lack of requirement for a specific sequence in the minihelix motif is paradoxical, because many RNAs that contain helices of similar length are not exported. To delineate the specific features of the minihelix motif, we constructed new mutants, derived from Stem17 and Stem20, to analyze their localization in COS1 cells.

First, a conserved feature of minihelices was the length of the stem. We thus created a set of artificial RNAs, which shortened the stem gradually from 20 to 12 bases (Fig. 5*A*). A stem of 12 bases was not exported, whereas a stem of 14 bases gave an intermediate phenotype (Fig. 5*B*).

A second characteristic of minihelices was base pairing of the RNA 5′-end, *i.e.* its first nucleotides with nucleotides close to the 3′-end (Fig. 1*A*). This suggested that the precise position of the RNA 5′- and 3′-ends could be critical for minihelix function. As shown in Fig. 5, a mutation designed to disrupt the first base pair of Stem20 (Fig. 5*A*, *MM1*) was sufficient to significantly decrease Stem20 export (Fig. 5*B* and Table I). Furthermore, mispairing of the first three base pairs completely blocked Stem20 export (Fig. 5*B, MM3*; and Table I). These results indicated that the RNA 5′-end had to be part of the minihelix in order to promote RNA export. Another set of mutants were designed to maintain the 5′-terminal base pairing, whereas the RNA 3′-end was displaced further downstream from the base of the stem. Insertion of 8 bases had little effect on export (Fig. 5*B, Xt8*), but an 18-base insertion blocked it completely (Fig. 5*B, Xt18*). This indicated that the minihelix should not only contain the RNA 5′-end, but should also have the 3′-end in its vicinity.

The last characteristic of the minihelix that we analyzed was its tolerance to bending. Indeed, mismatches such as the ones found in the terminal stem of VA1 allow stacking of the neighboring helices (41), but with flexibility and bending at the junction (42). As shown in Fig. 5*A*, we inserted bulges of 3 or 6 As in the middle of the stem of Stem20, because previous *in vitro* work predicted that these would create bends of 60° and 90°, respectively (42). The two mutant RNAs were still exported (Fig. 5*B, Stem-3A* and *Stem-6A*), indicating that artificial stems could tolerate strong bends and still be competent for export.

Altogether, these results showed that the minihelix had to meet some requirements in order to be a cytoplasmic localization motif. Beginning with the RNA 5′-end, the RNA 3′-end should be close to the base of the stem, and its length should be longer or equal to 14 nucleotides. To confirm that the effects we observed were due to variations in export efficiencies and not

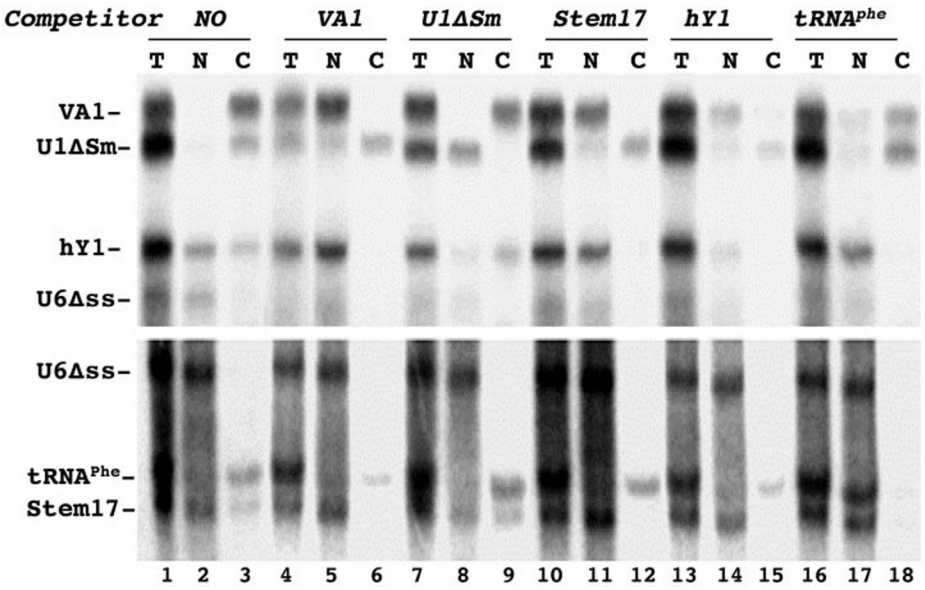

FIG. 4. **RNA export in the presence of competitors.** A mixture of 1.5 fmol of radiolabeled VA1, U1ΔSm, hY1, U6Δss, tRNA^{Phe}, and Stem17 was co-injected into oocyte nuclei in absence or in presence of 2.5 pmol of the indicated competitor. After injection, oocytes were incubated for 3 h at 21 °C, total (*T*), nuclear (*N*), and cytoplasmic (*C*) RNAs were then extracted and analyzed by polyacrylamide gel electrophoresis under denaturing conditions.

RNA stability, the expression levels and half-lives of several mutants were compared and showed no difference that could account for their opposite localization (Table I). Furthermore, mutants that had a short stem (Stem12), or that disrupted the base pairing of the RNA 5′-end (MM3), were not exported in *Xenopus* oocytes either (Fig. 3*B*).

Minihelix-containing RNAs are exported via a common export pathway. In order to investigate the relations between minihelices and other export pathways, we performed additional competition experiments in *Xenopus* oocytes. Among cellular RNAs, hY1 and tRNAs were of particular interest because these RNAs were both transcribed by pol III and displayed a terminal stem very similar to the one of VA1 (Fig. 7 and data not shown). As shown in Fig. 4, co-injection of an excess of VA1, Stem 17 or hY1 specifically inhibited the export of both VA1, Stem17, and hY1 (Fig. 4,). These cross-competitions were specific because none of these RNAs were able to inhibit export of U1ΔSm (*lanes 8* and *9*). Conversely, U1ΔSm did not compete in the export of VA1, Stem17, nor hY1. These results thus indicate that VA1, Stem17, and hY1 use the same nucleocytoplasmic export pathway, or at least a common limiting factor but do not share any export factor used for the nuclear export of U1.

Interestingly, export of VA1, Stem17, and hY1 was also partially inhibited by an excess of tRNA^{Phe} (Fig. 4, *lane 18*). However, export of tRNA^{Phe} was unaffected by an excess of VA1 (*lane 6*), Stem17 (*lane 12*), or hY1 (*lane 15*), whereas it was inhibited by the same amount of tRNA^{Phe} (*lane 18*). These results were consistent with earlier findings, because inhibition of hY1 export by excess of tRNA, but not the reverse, has been previously described (39). Taken together, this suggested that tRNAs may have some affinity for the minihelix *trans*-acting factors (see below).

Nuclear Export of Minihelices Is a Ran-dependent Process—To further characterize the export pathway of minihelices, we next analyzed whether RanGTP is required in this process. For this purpose, a mixture of U1ΔSm, VAΔIV, U6Δss, Stem20 and tRNA^{Phe} was co-injected into the nucleus of oocytes with either RanBP1 to reduce the nuclear concentration of RanGTP or with RanGAP from S. *pombe* (Rna1p) to deplete RanGTP from the nucleus (Fig. 6). As previously reported (55) nuclear injection of RanBP1 prevented the nuclear export of U1ΔSm without affecting the export of tRNA (*lanes 7–9 versus lanes 4–6*). This experimental condition also led to an inhibition of VAΔIV and Stem20 transport. In agreement with this result, nuclear injection of Rna1p completely blocked nuclear export of U1ΔSm, tRNA^{Phe}, and minihelices (*lanes 10–12 versus lanes 4–6*). These data indicate that nuclear export of minihelix-containing RNAs depends on nuclear RanGTP. To determine whether this export pathway requires GTP hydrolysis by Ran, we used a dominant-negative, GTPase-deficient mutant of Ran, RanQ69L. Nuclear injection of RanQ69L partially inhibited the nuclear export of U1ΔSm, VAΔIV, and Stem20 but did not affect tRNA transport (*lanes 13–14 versus lanes 4–6*) suggesting that nuclear export of minihelices likely depends on GTP hydrolysis by Ran.

DISCUSSION

Our analysis of VA1 export brings new insights into the mechanisms controlling the nucleocytoplasmic partitioning of pol III RNAs. We have discovered a novel and highly degenerate motif, the minihelix, that promotes cytoplasmic localization of pol III RNAs in vertebrates. In addition, the simplicity and the high degeneracy of this motif makes it very suitable to vehicle therapeutic RNAs, such as ribozymes, antisense or aptamers, into the cell cytoplasm.

The Minihelix Is a Novel RNA Export Motif, in Situ—detection of RNAs in transfected mammalian cells was used to show that the VA1 terminal stem is necessary and sufficient for cytoplasmic localization. Measurements of RNA half-lives suggested that the terminal stem did not selectively stabilize the RNA in the cytoplasm, but promoted RNA export. This point was further tested using nuclear injections in *Xenopus* oocytes. We found that indeed VA1 was gradually exported from the nucleus of *Xenopus* oocytes and that mutations that disrupted the terminal stem precluded its export. Furthermore, we showed that VA1 export could be specifically blocked by saturating amount of VA1 RNA.

Remarkably, the VA1 terminal stem can be replaced by a randomly chosen sequence without loss of activity. This observation demonstrates that the terminal stem does not require a specific sequence to be competent for the export. This point can be further reinforced by considering the high level of sequence variability observed among a large panel of adenovirus VA1 sequences. These stems, however, still required particular features to promote export. Indeed, artificial RNAs that had a stem shorter than 14 bases, or that disrupted the pairing of the RNA 5′-end, were unable to reach the cytoplasm and remained nuclear in mammalian cells. Importantly, these RNAs were also not exported in *Xenopus*. By testing a large panel of mutants, we found that in order to function the terminal stem

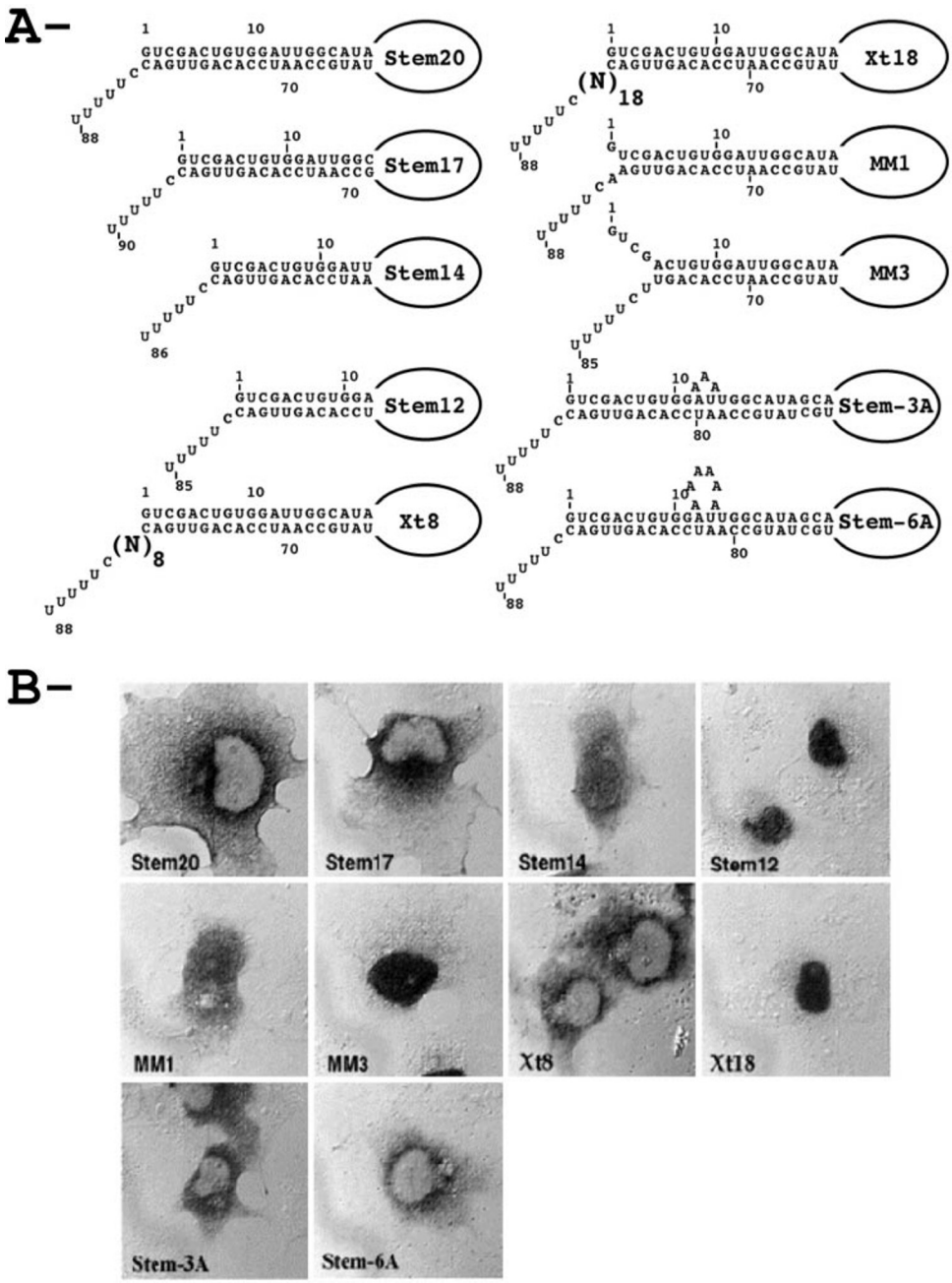

FIG. 5. **Terminal stems of random sequences promote export of pol III RNA.** *A*, structures of the artificial RNAs. These RNAs were derived from LacZ, and formed a loop of about 40 nucleotides closed by a terminal stem. Only the sequence and structure of the terminal stem are depicted. *B,* the intracellular localization of the artificial RNAs. The RNAs were expressed from the human U6 promoter, which is transcribed by pol III. COS1 cells were transiently transfected with the indicated plasmids, and the localization of the resulting RNA was analyzed by *in situ* hybridization. Each field represents 100 μm and shows a representative cell (see Table I for quantifications).

should start with the RNA 5′-end, should be longer than 14 nucleotides, and should have a 3–8 nucleotide long protruding 3′-end. This family of degenerated sequences thus defines a novel cytoplasmic localization motif, which we refer to as the minihelix motif.

An essential feature of the minihelix motif is its high degree of degeneracy. It not only lacks any sequence requirement, but it can also accommodate many distortions within the stem. The terminal stem of all VA1 RNAs contains two mismatches, and several VA1 mutants that we have generated contain slightly larger mismatches and, however, are still exported (Fig. 2). Also, bulges of 3 and 6 As could be inserted within the minihelix without preventing its export, when such bulges have been shown to induce bends of 60 and 90°, respectively (42).

Our study did not address a sequence requirement for the last 3′ bases, unpaired Us in all our mutants because it was not possible to mutate them since they acted as a pol III transcription termination signal. However, in the case of the hY1, which bears a functional minihelix motif (see below), these terminal Us promote nuclear retention via binding to the La protein, and do not export (39).

Minihelices Require a Common Limiting Transporter—By injection of competitor RNAs in *Xenopus* oocytes, we have characterized the minihelix export pathway. It was first observed that Stem17, an artificial RNA displaying a minihelix, could specifically compete with VA1 for export, and reciprocally. This suggests that export of unrelated minihelices relies on the same limiting transporter, which thus defines the minihelix pathway.

To determine the relationship between the minihelix and

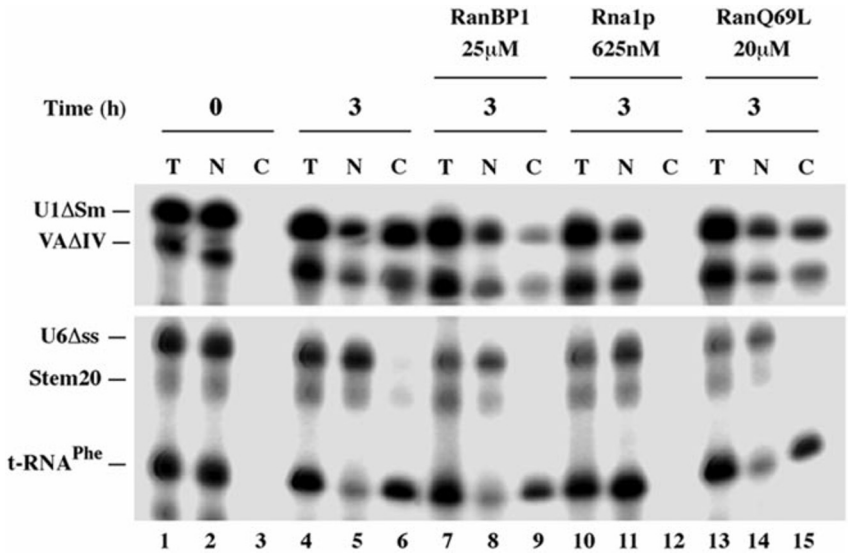

FIG. 6. **Nuclear export of minihelices is a Ran-dependent process.** A mixture of ^{32}P-labeled U1Δsm, VAΔIV, U6Δss, Stem20, and tRNA^{Phe} was co-injected into oocyte nuclei in the absence (*lanes 1–6*) or in the presence of RanBP1 (*lanes 7–9*), Rna1p (*lanes 10–12*), or RanQ69L (*lanes 13–15*) at the indicated concentrations in a total injection volume of 20 nl. After 0 (*lanes 1–3*) or 3 h (*lanes 4–15*) at 19 °C, total (*T*), nuclear (*N*), and cytoplasmic (*C*) RNAs were extracted and analyzed by polyacrylamide gel electrophoresis under denaturing conditions.

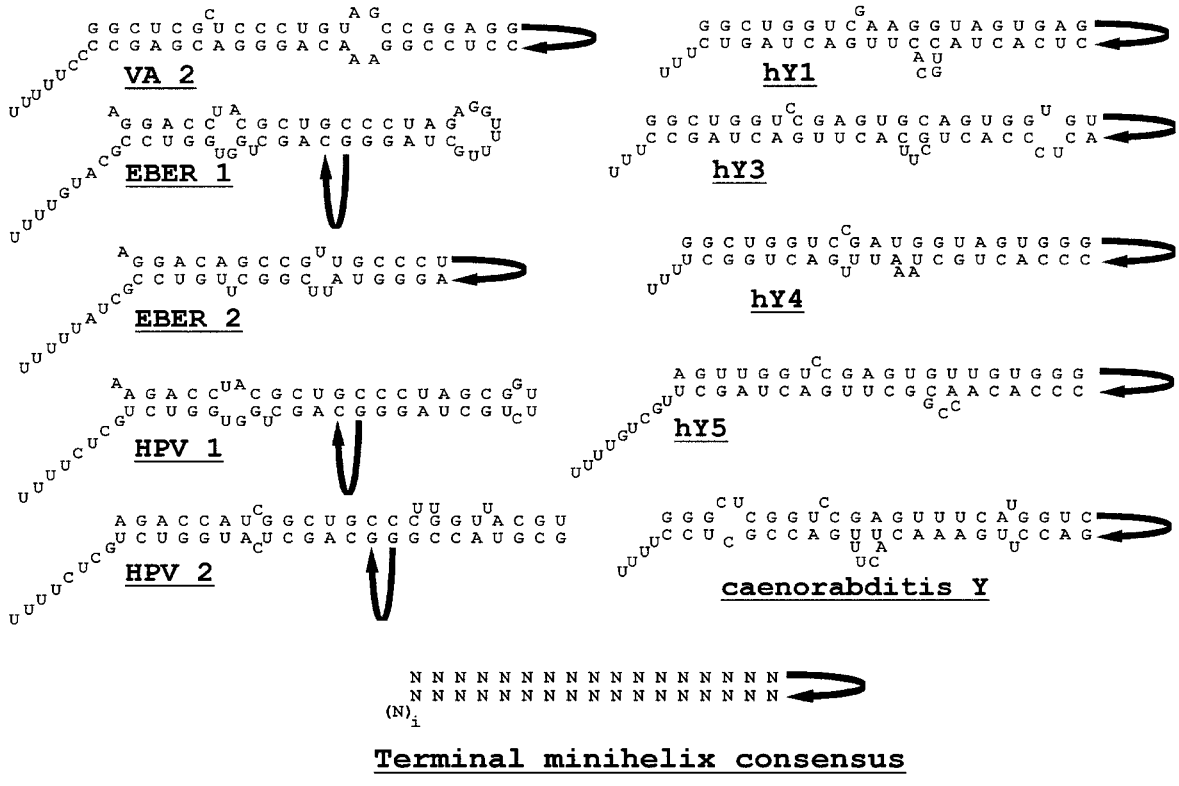

FIG. 7. **Structure of RNA potentially exported by the minihelix pathway.** The structure of the minihelix of several small cytoplasmic RNAs is pictured: adenovirus type 2 (VA2); Epstein-Barr virus (EBER1 and EBER2); *Herpesvirus* papio (HPV1 and HPV2); human Y1, Y3, Y4, and Y5 (hY1, hY3, hY4, and hY5); *Caenorhabditis* Y RNA. Only the sequence of the minihelix is shown, the rest of the RNA is schematized with a loop. The consensus for the minihelix motif is also shown. Note that this consensus tolerates bulges and mismatches. RNA sequences were retrieved from GenBank™ and folded using mfold software (53).

other export pathways, we tested the effect of other competitors, hY1, tRNA^{Phe} and U1ΔSm snRNA. Cross-competition occurred between VA1, Stem17, and hYI RNAs, indicating that VA1 and hY1 RNAs were likely to share the same nuclear export pathway or at least one common *trans*-acting factor. In contrast, U1ΔSm snRNA had no inhibitory activity on the export of either VA1, Stem17, or hY1 RNA, indicating that the minihelix pathway is distinct from that involving snRNAs and thus does not appear to involve CRM1. This was in agreement with previous results, which showed that hY1 was utilizing a pathway distinct from snRNA and leucine rich NES (39).

The relationship between the minihelix and tRNA pathways appears to be less clear. As previously observed for hY1, a tRNA competitor could block export of VA1 and Stem17; however, an excess of VA1 or Stem17 could not block export of tRNA^{Phe}. This could occur if tRNA^{Phe} could bind the minihelix transporter, whereas minihelices would not bind the tRNA transporter. The main pathway for tRNA export in *Xenopus* oocytes has been described to utilize Xpo-t, the tRNA exportin and *in vitro* binding assay has shown that human Xpo-t does not bind minihelices (11–13, 17). Thus, the minihelix export pathway is likely to be distinct from the one mediated by Xpo-t.

We have shown that minihelix export is blocked in the presence of the dominant negative GTPase-deficient mutant of Ran,

RanQ69L, or when RanGAP1 or RanBP1 are mislocalized. This indicates that minihelix export depends on Ran and suggests that this pathway involves an importin-β-related receptor. As a consequence, the minihelices receptor is likely a different TAP, a receptor involved in mRNA export that does not belong to the β-importin family and does not use Ran to interact with cargoes.

Natural RNAs Exported by the Minihelix Pathway—The high degeneracy of the minihelix motif raises the possibility that many pol III RNAs, from viral or cellular origin, could be exported through this export pathway. The precise definition of the minihelix motif suggests that candidate RNAs could be identified only on the basis of their structural features. As illustrated in Fig. 7, folding of the VA1 and VA2 homologs from simian and chicken adenoviruses fits the minihelix motif (25), suggesting that they could be exported by this pathway. The EBER and HPV RNAs, found in Epstein-Barr and herpes papio viruses, are similar to the VA RNAs and also display a terminal stem (43, 44). This stem, however, deviates from the minihelix consensus because the RNA 5′-end is left unpaired. Interestingly, we have shown that this kind of mutation reduces export, leading to an intermediary phenotype with the presence of such RNA both in nucleus and cytoplasm. This is in fact the intracellular distribution of the EBER RNAs (45), suggesting that an inefficient export signal could be used to regulate the localization of viral RNAs.

Several cellular RNAs transcribed by RNA pol III also fit the minihelix consensus. For instance, the Y RNAs that are components of Ro ribonucleoprotein particles and which form a family of small cytoplasmic RNAs conserved from worms to humans (Fig. 7 and Refs. 46, 47), have a minihelix motif. This structural similarity predicts that these RNAs could be exported by the minihelix pathway, an idea that is supported both by the fact that hY1 is a specific competitor for minihelices (this study) and by the requirement of an hY1 minihelix for export (39). Remarkably, a Y RNA that contains a minihelix has recently been found in Eubacteria (48). This suggests that Y RNAs may be widely distributed in the eukaryotic kingdom and that the minihelix pathway could be conserved among many eukaryotes.

Another intriguing possibility is that the minihelix pathway could export tRNAs. Indeed, a tRNA competitor could block minihelix export. Furthermore, tRNAs are L-shaped molecules, topologically similar to minihelices with a 90° bend, which are competent for export. The main pathway for tRNA export in *Xenopus* oocytes is mediated by the transporter Xpo-t, which does not recognize minihelices (11, 17). However, deletion of the yeast homolog of Xpo-t is known to be not lethal for the yeast, suggesting that tRNAs should be exported via an alternative export pathway. This subsidiary pathway is currently being characterized (49–51). Whereas export of tRNA by the minihelix pathway is speculative at this point, it is an attractive hypothesis because the high degeneracy of the motif would ensure export of all mature tRNA species independent of their primary sequence and subtle variations in three-dimensional architecture.

Acknowledgments—We thank Ian Mattaj and Michael Mathews for providing us with U6Δss and U1ΔSm constructs and VA1 mutants, respectively. We thank A. Wittinghofer for recombinant Rna1p and RanBP1 proteins. Special thanks are due to Magali Mailland for technical assistance.

REFERENCES

1. Custodio, N., Carmo-Fonseca, M., Geraghty, F., Pereira, H. S., Grosveld, F., and Antoniou, M. (1999) *EMBO J.* **18,** 2855–2866
2. Legrain, P., and Rosbash, M. (1989) *Cell* **57,** 573–583
3. Schmidt-Zachmann, M. S., Dargemont, C., Kuhn, L. C., and Nigg, E. A. (1993) *Cell* **74,** 493–504
4. Bataille, N., Helser, T., and Fried, H. M. (1990) *J. Cell Biol.* **111,** 1571–1582
5. Khanna-Gupta, A., and Ware, V. C. (1989) *Proc. Natl. Acad. Sci. U. S. A.* **86,** 1791–1795
6. Zasloff, M. (1983) *Proc. Natl. Acad. Sci. U. S. A.* **80,** 6436–6440
7. Dahlberg, J. E., and Lund, E. (1998) *Curr. Opin. Cell Biol.* **10,** 400–408
8. Izaurralde, E., and Adam, S. (1998) *RNA* **4,** 351–364
9. Mattaj, I. W., and Englmeier, L. (1998) *Annu. Rev. Biochem.* **67,** 265–306
10. Stutz, F., and Rosbash, M. (1998) *Genes Dev.* **12,** 3303–3319
11. Arts, G. J., Fornerod, M., and Mattaj, I. W. (1998) *Curr. Biol.* **8,** 305–314
12. Hellmuth, K., Lau, D. M., Bischoff, F. R., Kunzler, M., Hurt, E., and Simos, G. (1998) *Mol. Cell. Biol.* **18**, 6374–6386
13. Kutay, U., Lipowsky, G., Izaurralde, E., Bischoff, F. R., Schwarzmaier, P., Hartmann, E., and Gorlich, D. (1998) *Mol. Cell* **1,** 359–369
14. Hopper, A. K., Traglia, H. M., and Dunst, R. W. (1990) *J. Cell Biol.* **111,** 309–321
15. Matunis, M. J., Coutavas, E., and Blobel, G. (1996) *J. Cell Biol.* **135,** 1457–1470
16. Hamm, J., and Mattaj, I. W. (1990) *Methods Enzymol.* **181,** 273–284
17. Arts, G. J., Kuersten, S., Romby, P., Ehresmann, B., and Mattaj, I. W. (1998) *EMBO J.* **17,** 7430–7441
18. Lipowsky, G., Bischoff, F. R., Izaurralde, E., Kutay, U., Schafer, S., Gross, H. J., Beier, H., and Gorlich, D. (1999) *RNA* **5,** 539–549
19. Hamm, J., and Mattaj, I. W. (1990) *Cell* **63,** 109–118
20. Jarmolowski, A., Boelens, W. C., Izaurralde, E., and Mattaj, I. W. (1994) *J. Cell Biol.* **124,** 627–635
21. Wickens, M. P., and Gurdon, J. B. (1983) *J. Mol. Biol.* **163,** 1–26
22. Caceres, J. F., Screaton, G. R., and Krainer, A. R. (1998) *Genes Dev.* **12,** 55–66
23. Nakielny, S., and Dreyfuss, G. (1997) *Curr. Opin. Cell Biol.* **9,** 420–429
24. Pinol-Roma, S., and Dreyfuss, G. (1992) *Nature* **355,** 730–732
25. Ma, Y., and Mathews, M. B. (1996) *J. Virol.* **70,** 5083–5099
26. Mathews, M. B., and Shenk, T. (1991) *J. Virol.* **65,** 5657–5662
27. O'Malley, R. P., Mariano, T. M., Siekierka, J., and Mathews, M. B. (1986) *Cell* **44,** 391–400
28. O'Brien, C. A., Margelot, K., and Wolin, S. L. (1993) *Proc. Natl. Acad. Sci. U. S. A.* **90,** 7250–7254
29. Roe, B. A., Anandaraj, M. P., Chia, L. S., Randerath, E., Gupta, R. C., and Randerath, K. (1975) *Biochem. Biophys. Res. Commun.* **66,** 1097–1105
30. Barcellini, C. S., Fenard, D., Bertrand, E., Singer, R. H., Lefebvre, J. C., and Doglio, A. (1998) *Antisense Nucleic Acid Drug Dev.* **8,** 379–390
31. Bertrand, E., Castanotto, D., Zhou, C., Carbonnelle, C., Lee, N. S., Good, P., Chatterjee, S., Grange, T., Pictet, R., Kohn, D., Engelke, D., and Rossi, J. J. (1997) *RNA* **3,** 75–88
32. Terns, M. P., and Goldfarb, D. S. (1998) *Methods Cell Biol.* **53,** 559–589
33. Samarsky, D. A., Fournier, M. J., Singer, R. H., and Bertrand, E. (1998) *EMBO J.* **17,** 3747–3757
34. Mellits, K. H., and Mathews, M. B. (1988) *EMBO J.* **7,** 2849–2859
35. Mellits, K. H., Pe'ery, T., and Mathews, M. B. (1992) *J. Virol.* **66,** 2369–2377
36. Pe'ery, T., Mellits, K. H., and Mathews, M. B. (1993) *J. Virol.* **67,** 3534–3543
37. Cagnon, L., Cucchiarini, M., Lefebvre, J. C., and Doglio, A. (1995) *J. Acquir. Immune Defic. Syndr. Hum. Retrovirol.* **9,** 349–358
38. Hamm, J., and Mattaj, I. W. (1989) *EMBO J.* **8,** 4179–4187
39. Simons, F. H., Rutjes, S. A., van Venrooij, W. J., and Pruijn, G. J. (1996) *RNA* **2,** 264–273
40. Bhat, R. A., Metz, B., and Thimmappaya, B. (1983) *Mol. Cell. Biol.* **3,** 1996–2005
41. Kim, J., Walter, A. E., and Turner, D. H. (1996) *Biochemistry* **35,** 13753–13761
42. Zacharias, M., and Hagerman, P. J. (1995) *J. Mol. Biol.* **247,** 486–500
43. Howe, J. G., and Shu, M. D. (1988) *J. Virol.* **62,** 2790–2798
44. Rosa, M. D., Gottlieb, E., Lerner, M. R., and Steitz, J. A. (1981) *Mol. Cell. Biol.* **1,** 785–796
45. Schwemmle, M., Clemens, M. J., Hilse, K., Pfeifer, K., Troster, H., Muller, W. E., and Bachmann, M. (1992) *Proc. Natl. Acad. Sci. U. S. A.* **89,** 10292–10296
46. van Gelder, C. W., Thijssen, J. P., Klaassen, E. C., Sturchler, C., Krol, A., van Venrooij, W. J., and Pruijn, G. J. (1994) *Nucleic Acids Res.* **22,** 2498–2506
47. Van Horn, D. J., Eisenberg, D., O'Brien, C. A., and Wolin, S. L. (1995) *RNA* **1,** 293–303
48. Chen, X., Quinn, A. M., and Wolin, S. L. (2000) *Genes Dev.* **14,** 777–782
49. Grosshans, H., Simos, G., and Hurt, E. (2000) *J. Struct. Biol.* **129,** 288–294
50. Sarkar, S., and Hopper, A. K. (1998) *Mol. Biol. Cell* **9,** 3041–3055
51. Sarkar, S., Azad, A. K., and Hopper, A. K. (1999) *Proc. Natl. Acad. Sci. U. S. A.* **96,** 14366–14371
52. Mellits, K. H., Kostura, M., and Mathews, M. B. (1990) *Cell* **61,** 843–852
53. Zuker, M., and Jacobson, A. B. (1998) *RNA* **4,** 669–679
54. Klebe, C., Bishoff, F. R., Ponstingl, H., and Wittinghofer, A. (1995) *Biochemistry* **34,** 639–647
55. Izaurralde, E., Kutay, U., Von Kobbe, C., Mattaj, I. W., and Gšrlich, D. (1997) *EMBO J.* **16,** 65–35.-6547